

On the effect of coronal outflow on spectra formation in galactic black hole systems

A. Janiuk, B. Czerny, P.T. Życki

Nicolaus Copernicus Astronomical Center, Bartycka 18, 00-716 Warsaw, Poland

3 November 2018

ABSTRACT

We present the results of both analytical and numerical calculations of the amplitude of the reflection component in X-ray spectra of galactic black hole systems. We take into account the anisotropy of Compton scattering and the systematic relativistic bulk motion of the hot plasma. In the case of single scattering approximation the reflection from the disc surface is significantly enhanced due to the anisotropy of Compton scattering. On the other hand the calculations of multiple scattering obtained using the Monte Carlo method show that the anisotropy effect is much weaker in that case. Therefore, the enhanced backscattered flux may affect the observed spectra only if the disc surface is highly ionized, which reduces the absorption in the energy band corresponding to the first Compton scattering.

Key words: accretion, accretion discs – black hole physics – galaxies: active – X-rays: galaxies – X-rays: stars

1 INTRODUCTION

Hard X-ray spectra of the galactic black hole systems are well described by a power law primary emission along with the pronounced reflected component, which causes the observed flattening of the spectrum. The primary emission is likely to be produced by Compton upscattering of soft photons on thermal electrons in hot, optically thin medium close to a relatively cold accretion disc, being the source of seed photons for Comptonization (see e.g. review in Poutanen 1998). A fraction of the upscattered photons is directed towards the disk and can be reflected from its surface, giving the rise to reflected continuum and fluorescent iron line emission (Lightman & White 1988; George & Fabian 1991).

Observational data for Cyg X-1 and other black hole systems in their hard/low state show often rather hard spectra (photon spectral index $\Gamma \sim 1.5 - 1.9$; Poutanen et al. 1997; Gierliński et al. 1997; Dove et al. 1997; see also Poutanen 1998), while the amplitude of reflection R covers the broad range of values between 0 and 2. Moreover, R and Γ are correlated (Zdziarski, Lubiński & Smith 1999; Revnivtsev, Gilfanov & Churazov 1999), in the sense that the harder the spectrum, the smaller the amplitude of reflection. The correlation exists both within the low/hard state and when sources change their spectral state (Życki, Done & Smith 1998).

These observations cannot be explained by the model in which static, continuous corona covers the cold accretion disc, as it predicts the power law slope $\Gamma \geq 2$ (i.e. rather soft

spectra) and the reflection amplitude $R \sim 1.0$. Among the possible models, which could reproduce the reflection amplitude in the range $R = 0 - 1$ there are two competitive: (i) cold disc disrupted in the inner part (e.g. Poutanen, Krolik & Ryde 1997; Esin, McClintock & Narayan 1997) and (ii) a highly ionized, non-disrupted disc (Nayakshin, Kazanas & Kallman 2000; Ross, Fabian & Young 1999). Detailed shape of the reflected continuum depends on the geometry, ionization state and abundances of elements in the scattering medium. However, spectral fitting does not always allow to constrain these parameters independently. It is possible to explain the observed spectra of GBH in terms of weakly ionized, or neutral reflection from the disc which inner radius is of the order of $50 R_g$ (e.g. Done & Życki 1999 for the hard state of Cyg X-1), as well as with highly ionized reflection from the disc extending to the marginally stable orbit (as suggested by Ross et al. 1999 for the hard state of Cyg X-1; see also Done & Nayakshin 2000).

The third possible model, in which both the reflection amplitudes $R > 1$ and $R < 1$ are possible, is a mildly relativistic outflow/inflow in the corona (Beloborodov 1999). Relativistic aberration reduces the hard X-ray flux scattered towards the disc, which leads to reduction of the reflected component and the soft flux from reprocessing entering the corona. In order to obtain quantitative agreement with observed spectral indices and reflection amplitudes, the model requires additional reduction of the soft flux intercepted by the hot plasma. This leads to the 'active regions' geometry (e.g. magnetic flares above the disc; Haardt, Maraschi &

arXiv:astro-ph/0007070v1 6 Jul 2000

Ghisellini 1994) rather than a continuous corona. However, the coronal outflow may reproduce the reflection amplitude $R < 1$ and in order to obtain $R > 1$ an inflow of the plasma must be postulated.

In this article we reanalyze the non-static corona model, with plasma moving at relativistic speed in the direction perpendicular to the disc surface. We study the dependence of the amplitude of the reflection component on the bulk motion velocity, taking into account the thermal motion of electrons within the plasma determined by the electron temperature T_e and we discuss the resulting shape of the spectra. We also check if high reflection amplitudes ($R > 1$) might be explained in the frame of the outflow model but taking into account possible high ionization of the disc surface and the anisotropy of Compton scattering. We emphasize the importance of the first Compton scattering, which plays crucial role at lower energies. For highly ionized disc surface the effect of absorption by heavy elements is reduced and the reflected spectrum makes a substantial contribution to the total spectrum in the $\sim 0.5 - 5$ keV band. Therefore we present firstly the semi-analytical calculations in the approximation of single scattering, and after that we perform numerical simulations of multiple scattering, which is responsible for the power law shape of the hard X-ray tail.

The contents of the paper is as following. In Section 2 we analyze semi-analytically the amplitude of the reflection in a single scattering approximation (after Ghisellini et al. 1991) but taking into account anisotropy of scattering within the rest frame of the electron, describing the thermal motion without the assumption of highly relativistic beaming and incorporating the systematic bulk motion (outflow) of the corona. Since the effect of multiple scattering is essential in a real situation, in Section 3 we repeat the computations for a corona of a given optical depth and an electron temperature using a Monte Carlo method for both outwards and inwards directions of bulk velocity. The dependence of the reflection amplitude on the outflow velocity is presented in Section 3.1. The spectra resulting from Monte Carlo computations are presented in Section 3.2. The discussion of the results is given in Section 4.

2 SINGLE SCATTERING APPROXIMATION FOR THE AMPLITUDE OF REFLECTION

In this section we generalize the determination of the amplitude of the reflection component derived by Ghisellini et al. (1991) for a slab geometry of a hot corona and anisotropic soft photon input from underlying disc. Those results were obtained assuming isotropic electron scattering in the rest frame of an electron and relativistic chaotic motion of electrons. We introduce subsequently the anisotropy of the Thomson cross-section (Section 2.1), we relax the assumption that the thermal motion of the plasma is relativistic (Section 2.2), and finally we introduce the systematic bulk motion of the corona (Section 2.3).

We show, that including the effect of anisotropic soft photon distribution in Compton scattering process the reflection amplitude $R \geq 2$ can be obtained. It's value is somewhat larger when the angular dependence of Thomson cross-section is taken into account. On the other hand for low electron velocities ($\gamma < 2$) the angular distribution of

scattered radiation becomes important and the value of R is reduced. Adding the systematic coronal outflow reduces the anisotropy effect only in the range of high bulk velocities. However all these results stand mostly for the first scattering, while for the multiple scattering in the cloud of optical depth $\tau \sim 1$ the reflection is weaker (see Section 3).

2.1 The effect of angular dependence of the Thomson cross-section

In this section we calculate the power of Compton radiation scattered by electrons with isotropic relativistic velocity field $v = \beta c$, $\beta \sim 1$. This approach is appropriate for a non-thermal plasma. The radiation field is anisotropic and incoming photons subtend a restricted solid angle. We assume the geometry is the same as in Ghisellini et al. (1991). However, in our calculations we take into account the angular dependence of Thomson cross-section (Rybicki & Lightman, 1979). Therefore the emitted power is given by

$$P(\alpha, \gamma) = \frac{3}{8} \frac{P_{\text{iso}}}{(1 + \beta^2/3)} \int_{\phi_{\text{min}}}^{2\pi - \phi_{\text{min}}} d\phi \int_{\theta_{\text{min}}}^{\theta_{\text{max}}} (1 - \beta \cos \theta)^2 (1 + \cos^2 \theta) \sin \theta d\theta \quad (1)$$

Here P_{iso} is the power of isotropic emission and $P(\alpha)$ is the power of radiation scattered by electron of the angle α between its velocity and the axis of symmetry of incoming photons. The limits θ_{min} , θ_{max} and ϕ_{min} are functions of α and are given by equations (see Ghisellini et al., 1991):

$$\begin{aligned} \theta_{\text{min}} &= \max(0, \alpha - \pi/2) \\ \theta_{\text{max}} &= \min(\alpha + \pi/2, \pi) \end{aligned} \quad (2)$$

$$\phi_{\text{min}} = \begin{cases} 0 & \text{for } 0 < \theta < \pi/2 - \alpha \\ & \text{or } 3\pi/2 - \alpha < 0 < \pi \\ \arccos[(\tan \theta \tan \alpha)^{-1}] & \text{otherwise} \end{cases}$$

Here we follow the assumption of Ghisellini et. al (1991), that all photons are emitted in the direction of electron's velocity. This is justified in the case of $\gamma \gg 1$, when the direction of the motion of an electron (i.e the angle α) can be identified with the viewing angle. In Figure 1 we plot the ratio of the total power emitted by electrons moving downwards to that of electrons moving upwards:

$$R(\gamma) = \frac{\int_{\pi/2}^{\pi} P(\alpha) \sin(\alpha) d\alpha}{\int_0^{\pi/2} P(\alpha) \sin(\alpha) d\alpha} \quad (3)$$

It is worth seeing that this ratio saturates for large γ at the value of $R \sim 2.55$, which is somewhat larger than that obtained under assumption of $d\sigma/d\Omega = \sigma_T/4\pi$ ($R \sim 2.2$). This result might be of possible importance for non-thermal Comptonization models. It seems however to be in conflict with the recent results of spectral fitting of the data for the soft state of Cyg X-1 (Gierliński et al. 1999).

In Figure 2 we plot the ratio of the power emitted downwards to that emitted by electron moving in one particular direction, given by

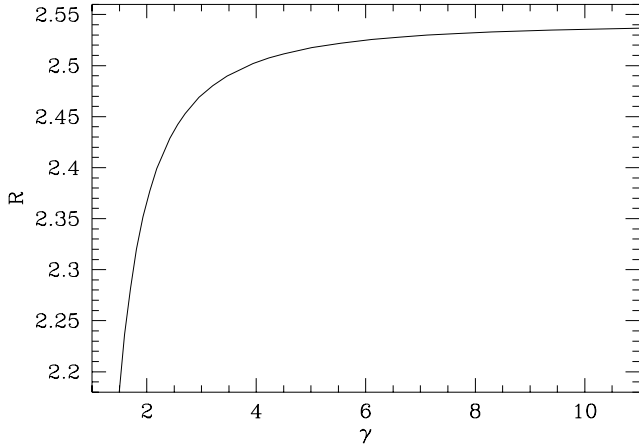


Figure 1. The ratio of the total power emitted by electrons moving downwards to that of moving upwards as a function of electron's Lorentz factor γ .

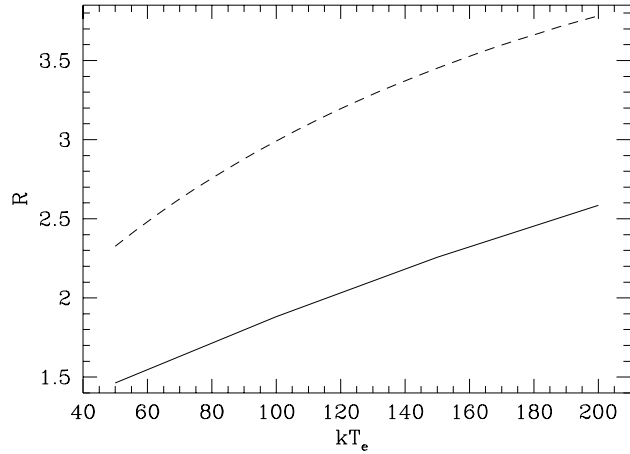


Figure 2. The ratio of the total power emitted by electrons moving downwards to that of electron moving in one particular direction, as a function of electron temperature kT [keV], for an inclination angle $\alpha = 30^\circ$, under the assumption of efficient beaming (dashed line), and for the same inclination angle ($i = 30^\circ$) but averaged over the whole range of electron's velocity direction (solid line).

$$R(\alpha, kT) = \frac{\int_{\pi/2}^{\pi} P(\alpha) \sin(\alpha) d\alpha}{P(\alpha)}. \quad (4)$$

This can be identified with the reflection amplitude seen by the observer with the viewing angle α . We plot the result versus the electron temperature instead of γ in order to expose better the lower velocity part of the curve but we remind that those results (dashed line) are not supposed to be accurate for not very highly relativistic velocities. We see that for low inclination angle the expected enhancement of the reflection is very large, up to a factor 3.5 for typical plasma temperatures.

2.2 The effect of mildly relativistic thermal motion

If the plasma is rather thermal than non-thermal, the electron velocity is only mildly relativistic and the assumption of all the emission being beamed in the direction of motion of an electron used in Section 2.1 is not valid. Therefore, in this section we consider the angular distribution of the scattered radiation, given by

$$P(\alpha, \gamma, \Theta_{\text{out}}) = \frac{P(\alpha, \gamma)}{2\gamma^4(1 + \beta \cos \Theta_{\text{out}})^3} \quad (5)$$

where $\Theta_{\text{out}} = \pi$ means scattering in the direction of electron's movement. The accretion disc receives a fraction of scattered radiation that depends on the direction and velocity of electron

$$P_{\text{disc}}(\alpha, \gamma) = \int_{\Theta_{\text{out}}^{\text{min}}}^{\Theta_{\text{out}}^{\text{max}}} \int_{\phi_{\text{out}}^{\text{min}}}^{2\pi - \phi_{\text{out}}^{\text{min}}} P(\alpha, \gamma, \Theta_{\text{out}}) \sin \Theta_{\text{out}} d\Theta_{\text{out}} d\phi_{\text{out}} \quad (6)$$

where $\Theta_{\text{out}}^{\text{max}}$, $\Theta_{\text{out}}^{\text{min}}$ and $\phi_{\text{out}}^{\text{min}}$ are given by equations (2).

The viewing angle i in this case cannot be identified with the direction of electron motion given by α . Instead, we have a relation

$$\cos \Theta_{\text{out}} = -(\sin i \sin \varphi \sin \alpha + \cos i \cos \alpha). \quad (7)$$

Here α and φ determine the electron's velocity vector direction:

$$\vec{v} = v(\cos \varphi \sin \alpha, \sin \varphi \sin \alpha, \cos \alpha) \quad (8)$$

In Figure 3 we show the assumed geometry scheme. Note, that the angle Θ_{out} is measured from the vector $-\vec{v}$ to the direction of emitted photon, and therefore we keep the integration limits given by equations (2) unchanged (see also Fig. 1 and Fig. 2 in Ghisellini et al. 1991).

We calculate the reflection amplitude averaged over the whole range of α and φ as a function of electron velocity and viewing angle, according to the formula

$$R(\gamma, i) = \frac{1}{2\pi} \frac{\int_0^\pi \int_0^{2\pi} P_{\text{disc}}(\alpha, \gamma) \sin \alpha d\alpha d\varphi}{\int_0^\pi \int_0^{2\pi} P(\alpha, \gamma, \Theta_{\text{out}}(\alpha, \varphi, i)) \sin \alpha d\alpha d\varphi}. \quad (9)$$

In Figure 4 we plot the reflection amplitude as a function of γ for three different values of viewing angle. The plot for an inclination $i = 60^\circ$ roughly corresponds to the value averaged over all inclinations, as presented in Figure 1 for non-thermal plasma. We see that the anisotropy is only slightly reduced if the total collimation assumption is relaxed. This effect is mostly seen in Figure 2 where we present with the solid curve low velocity (moderate temperature) tail of the distribution.

2.3 Mildly relativistic bulk motion

In this section we assume that bulk velocity vector is perpendicular to the disc surface and directed outwards. We calculate the net electron velocity as a sum of thermal chaotic motion and systematic (bulk) outflow. The angle between the net velocity vector and vertical axis, α' , is connected with angle α via relativistic velocity transformation. Therefore the net Lorentz factor, γ' , depends on the angle α' as well

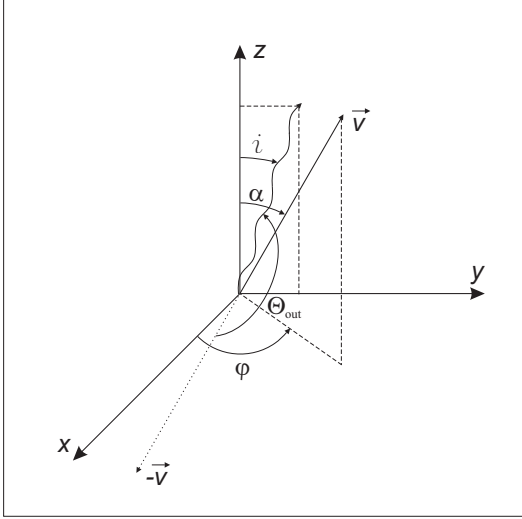


Figure 3. The assumed geometry scheme. The electron is in the center of the reference frame and has the velocity \vec{v} at the inclination α to the symmetry axis of the disc and at the angle φ measured in the disc plane. The photon is emitted at the angle i to the disc axis, and at the angle $(\Theta_{\text{out}} - \pi)$ to the electron's velocity vector.

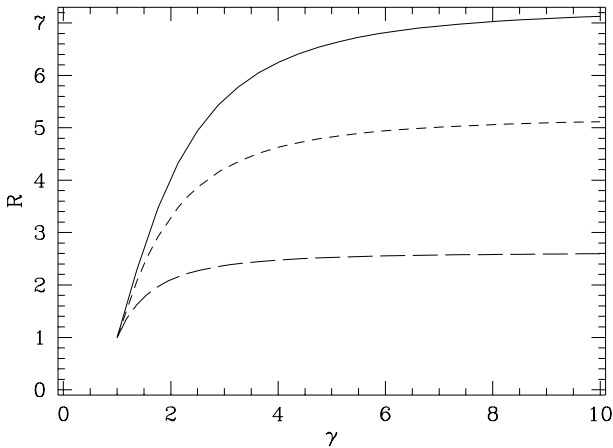


Figure 4. The reflection amplitude for the viewing angle $i = 0$ (solid line), 30° (short-dashed line) and 60° (long-dashed line) as a function of electron's Lorentz factor γ in case of pure thermal motion.

as on bulk and thermal velocities. In this case the amount of reflection is given by:

$$R(\beta_{\text{bulk}}, \beta_{\text{therm}}, i) = \frac{1}{2\pi} \times \frac{\int_0^\pi \int_0^{2\pi} P_{\text{disc}}(\alpha', \beta_{\text{bulk}}, \beta_{\text{therm}}) \sin \alpha' d\alpha' d\varphi'}{\int_0^\pi \int_0^{2\pi} P(\alpha', \beta_{\text{bulk}}, \beta_{\text{therm}}, \Theta_{\text{out}}(\alpha', i)) \sin \alpha' d\alpha' d\varphi'} \quad (10)$$

In Figure 5 we plot the dependence of the amount of reflection on the bulk velocity to the light velocity ratio, β_{bulk} , for different values of electron temperature β_{therm} and

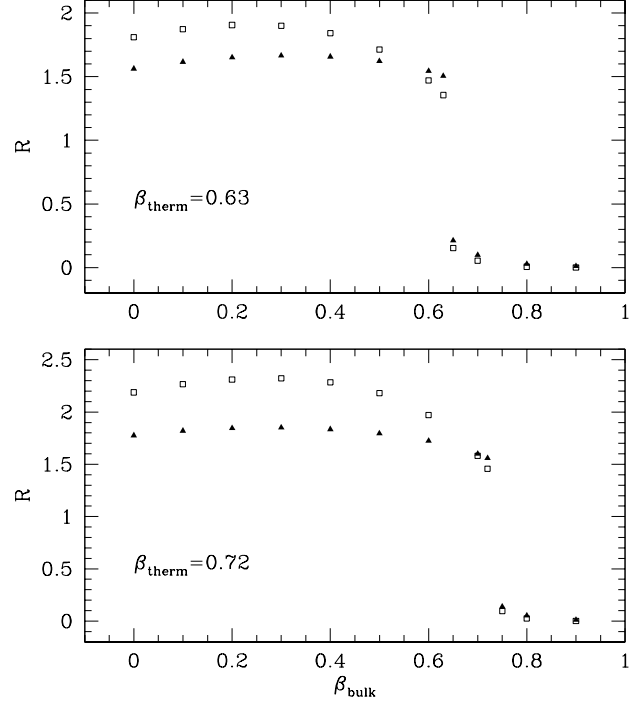


Figure 5. The reflection amplitude for the viewing angle $i = 0^\circ$ (boxes) and $i = 45^\circ$ (triangles) as a function of β_{bulk} for electron temperature $\beta_{\text{therm}} = 0.63$ (top panel) and $\beta_{\text{therm}} = 0.72$ (bottom panel).

viewing angle i . The electron temperature corresponds to a single value of electron velocity, as for velocity distribution the analytic approximation would not work.

In the case of $v_{\text{therm}} = 0$ we obtain the same solution as in Beloborodov (1999). In Figure 6 we plot this solution, calculated for different viewing angles.

The comparison of Figures 6 and 5 shows that single scattering approach predicts very strong dependence of the amplitude of reflection on the plasma temperature due to anisotropy of the Compton scattering. When the thermal motions are important ($v_{\text{therm}}/c \approx \beta_{\text{bulk}}$) the first reflection is significantly enhanced, by a factor of a two, and the higher the temperature the stronger the effect. The values of the amplitude of reflection cover the whole range between 0 and ~ 2 for outflow solutions ($\beta_{\text{bulk}} > 0$).

The effect of reflection enhancement drops rapidly when the bulk velocity is dominant ($\beta_{\text{bulk}} > v_{\text{therm}}/c$). In this case the maximum angle α' is much smaller than π and the integration limits in the equation (10) must be changed. The reflection amplitude increases then with the value of assumed viewing angle i , while in the case of more significant thermal motion the trend is opposite.

3 REFLECTED SPECTRA FROM MONTE CARLO SIMULATIONS

The roughly power law shape of the primary emission component in X-ray spectra in GBH is most likely due to the effect of multiple scatterings within the hot plasma.

It is well known from analytical solutions and Monte

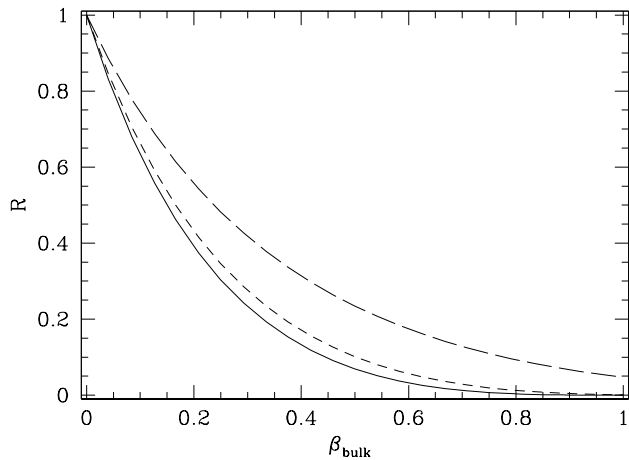


Figure 6. The reflection amplitude for the viewing angle $i = 0^\circ$ (solid line), 30° (short-dashed line) and 60° (long-dashed line) as a function of β_{bulk} for pure bulk motion.

Carlo simulations that the contribution of the first scattering to the total spectrum is rather specific (see Stern et al. 1995, Svensson 1996, Haardt, Maraschi & Ghisellini 1997). It means, that when the hard X-ray spectrum forms via multiple scatterings, only the first one is influenced by the anisotropy of seed photon distribution. This is the reason why any anisotropy effects are present in the low energy part of the spectrum. In the thermal medium, even for small optical depths, the power law spectrum is shaped by multiple scatterings. Therefore the semi-analytical computations, dealing with the first scattering process, in the case of both thermal and systematic bulk motion of the electrons within the corona can only serve as a guide and a help to understand the numerical results. The fully reliable answer can only be provided by full Monte Carlo simulations of the Comptonization process within the corona.

In this Section we compute the amplitude of the Compton reflected component using a Monte Carlo comptonization code and we show the corresponding spectra. We concentrate on highly ionized reflector, as the approximations used in Beloborodov (1999) may not be valid in that case. The code employs standard algorithms for simulating the inverse Compton scattering, and it was written following descriptions by Pozdnyakov, Sobol & Sunyaev (1983) and Górecki & Wilczewski (1984). Modifications to the code necessary to implement the bulk motion are described in Appendix A. Following Beloborodov (1999) we assume that the comptonizing region as a whole is stationary and its geometry is that of a slab.

3.1 Reflection amplitude

The bulk velocity vector is assumed perpendicular to the plane of the disc but the direction of the velocity can be both outwards and towards the disc. The disc is a source of soft photons for the comptonization. Photons backscattered from the cloud form radiation illuminating the disc. The usual Compton reflection process is then simulated by another Monte Carlo routine (Życki & Czerny 1994), assuming the abundances given in Morrison & McCammon (1983). The opacities were computed using the code de-

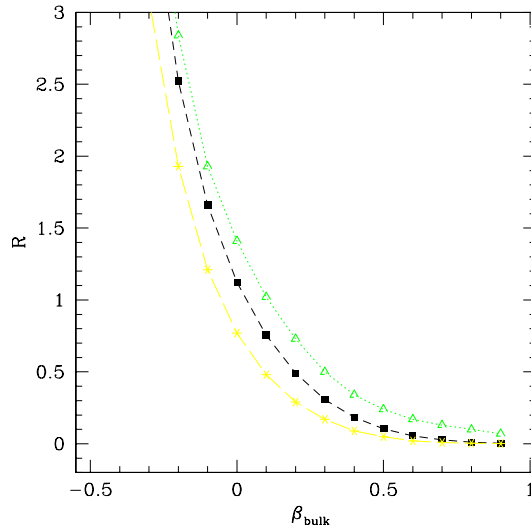


Figure 7. Amplitude of the Compton-reflected component as a function of the bulk outflow velocity, β_{bulk} , computed using the Monte Carlo method for multiple scattering in the plasma of optical depth $\tau_{\text{es}} = 0.8$ and electron temperature $kT_e = 100$ keV. Open triangles indicate the results for the inclination angle $\cos i = 0.3$, stars mark the results for $\cos i = 0.9$, and solid squares result from the angle averaged spectrum.

scribed in Done et al. (1992) for the ionization parameter $\xi \equiv F_X/(n_e r^2) = 10^4$. Further scattering of the reflected photons in the hot comptonizing cloud is not considered, since the intercepted fraction would be geometry-dependent (e.g. factor μ_s in Beloborodov 1999).

The reflection amplitude R is defined here (cf. Beloborodov 1999 and Section 2.3), as the ratio of the energy integrated fluxes:

$$R(\beta_{\text{bulk}}) = \frac{F_{\text{back}}(\beta_{\text{bulk}})}{F_{\text{dir}}(\beta_{\text{bulk}}, i)}. \quad (11)$$

Here F_{dir} is the flux directly escaping from the comptonizing cloud towards an observer, at the inclination angle i , and F_{back} is the flux directed towards the disc. We note that our definition of R would only be equivalent to that used in spectral fitting, if the shapes of spectra used in models fit to the data were exactly the same as in our simulations (for both the primary and the reflected components). Since this is not necessarily the case in practice, translating an amplitude R inferred from spectral modelling to a bulk velocity may not be accurate.

The parameters of the comptonizing cloud: the electron temperature kT_e and optical depth τ_{es} are chosen so that the resulting comptonized spectra correspond to typical spectra of GBH. Figure 7 shows the resulting amplitude of the reprocessed component as a function of the plasma bulk velocity β_{bulk} .

Comparison of the Figures 7 and 5 shows that the enhancement of the reflection due to the anisotropy of the first scattering is sharply reduced if the subsequent scatterings are taken into account. Only for rather high inclination angles is the obtained reflection amplitude larger than 1.0 for $\beta_{\text{bulk}} > 0$, as the larger the viewing angle, the fewer photons are able to escape from the slab towards the observer. This means, in particular, that bulk velocities directed *to-*

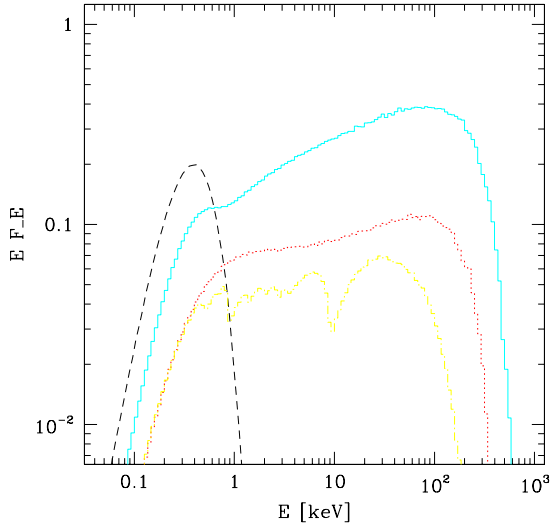


Figure 8. Comptonized spectra resulting from the outflowing corona model obtained by Monte Carlo simulations. Parameters were chosen so that the spectra correspond to typical spectra of low/hard state of GBH: $kT_e = 100$ keV, $\tau_{es} = 0.8$. The bulk velocity is $\beta_{\text{bulk}} = 0.3$. The dashed line represents the soft photon input, solid line shows the comptonized continuum scattered towards the observer (angle averaged), the short-dashed line shows the backscattered spectrum and the short-long-dashed line represents the reflected spectrum for ionization parameter, $\xi = 10^4$.

wards the disc are still necessary in some cases in order to explain full range of the Γ - R relation found by Zdziarski et al. (1999), as the enhancement of flux towards the disc due to plasma bulk motion is required to explain $R > 1$ seen in some sources.

3.2 Radiation spectra of outflowing corona

In Figure 8 we present an example of the overall spectrum calculated from the model of the outflowing corona. We choose the following values for the model parameters: $kT_e = 100$ keV, $\tau = 0.8$, $kT_0 = 0.1$ keV and the bulk velocity $\beta_{\text{bulk}} = 0.3$. Adopted soft photon temperature corresponds to a typical value for galactic black holes. Such a parameterization is convenient if we do not consider the energy balance within the corona. We assume that the corona is a continuous medium, i.e. we neglect the clumpiness of the corona described by the parameter μ_s in the model of Beloborodov (1999) since we also neglect the secondary reprocessing of the reflected component through the corona.

The continuous line shows the radiation emitted towards an observer (averaged over the entire hemisphere, roughly corresponding to an inclination of 60°) while the short-dashed line shows the component backscattered towards the disk. Since the first scattering dominates soft X-ray band for galactic sources, the backscattered radiation in this band is enhanced, as predicted by analytical results presented in Section 2. However, hard X-ray part is dominated by multiple scattered photons, anisotropy effect is smeared off and the backscattered component is not enhanced in this band. The net effect is therefore the systematic difference between the spectral slope of the back-scattered radiation

and forward-scattered radiation. This effect was discussed for a corona without a bulk motion in a number of papers (e.g. Stern et al. 1995). Therefore, the continuum formed in the corona and emitted towards an observer is slightly curved, particularly in the soft X-ray band, instead of being a simple power law with a high energy cut-off, as frequently assumed in spectral analysis of the data.

The backscattered continuum is subsequently reflected by the disk surface which in our calculations is assumed to be ionized ($\xi = 10^4$). We show this spectral component in the Figure 8.

The reflected component in the outflowing corona model is again partially reprocessed by the corona. The effect depends on the corona clumpiness since only a fraction of radiation μ_s (following the notation of Beloborodov, 1999) would pass again through the hot plasma. In the present paper we neglect this secondary reprocessing since it is essential only if μ_s is close to 1 and the optical depth is close to 1. However, in detail modeling this effect should be rather taken into account.

4 DISCUSSION

It is generally assumed that in galactic X-ray sources and active galactic nuclei soft X-ray radiation originates from the geometrically thin and optically thick accretion disc while the hard flux is produced by Comptonization in optically thin plasma outside the disc. Part of the hard X-ray flux that is directed towards the observer is detected in the form of power law continuum and the part of the flux scattered back to the disc surface produces so called 'reflection hump' in the spectrum over 10 keV (Lightman & White 1988; Pounds et al. 1990; Done et al. 1992) as well as the iron K_α line near 6.4 keV (Życki & Czerny 1994).

The observed values of the amplitude of the reflection component cover broader range than initially expected ($R \sim 1$ for AGN in Pounds et al. 1990). For some X-ray sources the observed reflection seems to be weak, which was modelled either by the disruption of the inner disc and X-ray irradiation of its outer parts, or by the high ionization state of illuminated medium, which results in steepening of the reflected continuum and makes it indistinguishable from the primary power law (Ross et al. 1999).

Both interpretations can explain the observed correlation between R and Γ . In the model with a disrupted cold disc partially overlapping the innermost hot flow the observed correlation is due to radiative coupling of the two components, as the amount of overlap varies (Zdziarski et al. 1999). In the model with strongly ionized disc surface the correlation is governed by the variable optical depth of the ionized scattering layer (Nayakshin et al. 2000), which determines the effective albedo of the disc and the soft flux from thermalized fraction of the illuminating X-rays. Both models can explain the reflection amplitude values $R \leq 1$.

However, the strength of reflection was for some sources found to be $R > 1$, which may either indicate that reflecting medium subtends a solid angle larger than 2π , or that the radiation directed towards the disc is enhanced. The latter is possible when the scattering process is anisotropic or may be due to the velocity of systematic bulk motion directed towards the disc.

In this article we show that the anisotropy effect is important mostly for the first scattering and weakens in numerical Monte Carlo simulations performed for multiple scattering in the plasma parameterized by optical depth and electron temperature. The maximum amplitude reached in the case of highly ionized reflector is only $R \sim 1.1$. Therefore, the systematic mildly-relativistic motion towards the disc, or the 'coronal inflow', is required to explain the higher values of R . On the other hand, in order to produce $R > 1$ in the disrupted disc model it would be necessary to allow for reflection from outer regions of a thickened disc (e.g. Shakura & Sunyaev 1973) and/or from the dusty/molecular torus around central black holes of AGN. Since the absorption of irradiating X-rays below ~ 5 keV is reduced for a highly ionized disc surface, the reflected photons may contribute to the soft X-ray excesses observed in the spectra of GBH in the hard/low state (Cyg X-1; Di Salvo et al. 1999, and in preparation). We show that this contribution is higher when the radiation backscattered to the disc is enhanced as a result of the anisotropy of the first scattering.

The hard to low state transition characteristic for many accreting black hole systems is in the 'disc plus sphere' model connected with the change of the inner radius of the cold disc. In the hard spectral state the cold disc is pushed outward while the hot inner plasma is responsible for hard X-ray radiation. In the soft state the thermal disc emission dominates as the cold disc extends almost to the marginally stable orbit. However, the physical mechanism of such behaviour is currently unclear. In the outflowing corona model the outflow velocity is the basic control parameter. The hard spectral state would then correspond to rapid coronal expansion, while the spectrum with dominating soft component would be produced during the vertical collapse of the hot gas. Again the physical mechanism of such dependence is unclear, and in particular it is unclear how the required changes of either R_{in} or β_{bulk} could be driven by changing accretion rate.

In conclusion, the basic predictions of all the proposed models are similar and only detailed computations of spectral and temporal behaviour and comparison with the high quality data, as expected from Chandra and XMM, may allow for a distinction between them.

ACKNOWLEDGMENTS

This work was supported in part by grant 2P03D01816, 2P03D01718 and 2P03D01519 of the Polish State Committee for Scientific Research.

REFERENCES

- Beloborodov A.M., 1999, ApJ, 510, L123
 Di Salvo T., Done C., Życki P.T., Burderi L., Robba N.R., 1999, Astrophysical Letters and Communications, 38, 261
 Done C., Mulchaey J.S., Mushotzky R.F., Arnaud K.A., 1992, ApJ, 395, 275
 Done C., Życki P. T. 1999, MNRAS, 305, 457
 Done C., Nayakshin S. 2000, ApJ, submitted

- Dove J.B., Wilms J., Maisack M., Begelman M.C., 1997, ApJ, 487, 759
 Esin A. A., McClintock J. E., Narayan R., 1997, ApJ, 489, 865
 George I.M., Fabian A.C., 1991, MNRAS, 249, 352
 Ghisellini G., George I.M., Fabian A.C., Done C., 1991, MNRAS, 248, 14
 Gierliński M., Zdziarski A. A., Done C., Johnson W. N., Ebisawa K., Ueda Y., Haardt F., Phlips B. F., 1997, MNRAS, 288, 958
 Gierliński M., Zdziarski A. A., Poutanen J., Coppi P. S., Ebisawa K., Johnson W. N., 1999, MNRAS, 309, 496
 Górecki A., Wilczewski W., 1984, Acta Astron., 34, 141
 Haardt F., Maraschi L., Ghisellini G., 1994, ApJ, 432, L95
 Haardt F., Maraschi L., Ghisellini G., 1997, ApJ, 476, 620
 Janiuk, A., Życki, P.T., Czerny, B., 2000, MNRAS (in press)
 Lightman A.P., White T.R., 1988, ApJ, 335, 57
 Morrison R., McCammon D., 1983, ApJ, 270, 119
 Nayakshin S., Kazanas D., Kallman T., 2000, ApJ, in press, (astro-ph/9909359)
 Pounds K.A., Nandra K., Steward G.C., George I.M., Fabian A.C., 1990, Nat., 344, 132
 Poutanen J., Krolik J.H., Ryde F., 1997, MNRAS, 292, L21
 Poutanen J., 1998, in Abramowicz M.A., Björnsson G., Pringle J.E. eds, Theory of Black Hole Accretion Discs, Cambridge Univ. Press, p. 100
 Pozdnyakov L.A., Sobol I.M., Sunyaev R.A., 1983, ASPR, 2, 189
 Press W.H., Teukolsky S.A., Vetterling W.T., Flannery B.P. 1992, "Numerical Recipes in Fortran", CUP
 Revnivtsev M., Gilfanov M., Churazov E., 1999, A&A Letters, submitted, (astro-ph/9910423)
 Rybicki G.B., Lightman A.P., 1979, "Radiative Processes in Astrophysics", Wiley, New York
 Ross R.R., Fabian A.C., Young A.J., 1999, MNRAS, 306, 461
 Shakura N.I., Sunyaev R.A., 1973, A&A, 24, 337
 Stern, B.E., Poutanen, J., Svensson, R., Sikora, M., Begelman, M.C., 1995, ApJ, 449, L13
 Svensson, R., 1996, ApJS, 120, 475
 Zdziarski A.A., Lubiński P., Smith D.A., 1999, MNRAS, 303, L11
 Życki P.T., Czerny B., 1994, MNRAS, 266, 653
 Życki P.T., Done C., Smith D., 1998, ApJ, 496, L25

APPENDIX A: THE MONTE CARLO CODE

Our initial comptonization code was written following closely descriptions given by Pozdnyakov, Sobol & Sunyaev (1983) and Górecki & Wilczewski (1984), and applied to model X-ray spectra of accretion disc with accreting advective corona by Janiuk, Życki & Czerny (2000). In order to include the effect of bulk motion of the plasma, we needed to make two major modifications.

Firstly, the average scattering cross section has to be modified. The escape probability of a photon is given by

$$P(d) = \exp\left(-\int_0^d N_e(\sigma) dl\right), \quad (\text{A1})$$

where $N_e = \int N(\mathbf{v}) d^3v$ is the electron density, $N(\mathbf{v})$ is the electron velocity distribution, d is the distance to the cloud boundary along the direction of photon motion, Ω , and

$$\langle\sigma\rangle = \frac{1}{N_e} \int N(\mathbf{v})(1 - \mathbf{v} \cdot \Omega/c)\sigma(x)d^3v \quad (\text{A2})$$

is the scattering cross section averaged over $N(\mathbf{v})$. Here

$$x = 2\frac{h\nu}{m_e c^2}\gamma(1 - \mathbf{v} \cdot \Omega/c) \quad (\text{A3})$$

is the energy of an incoming photon in the electron rest frame, γ is the Lorentz factor and $\sigma(x)$ is the Klein-Nishina cross section. For an isotropic $N(\mathbf{v})$ e.g. Maxwell distribution, $\langle\sigma\rangle$ is a function of photon energy only (for a given kT_e).

With the non-zero bulk velocity we cannot use the method presented by Pozdnyakov et al. (1983) to evaluate the integral in Eq. (A2), since $N(\mathbf{v})$ is no longer isotropic. The presence of the specific direction – the bulk velocity vector $\boldsymbol{\beta}$ – introduces an additional angular dependence of $\langle\sigma\rangle$. We now have to compute the integral as in Eq. (A2) but with \mathbf{v} in the dot-product $\mathbf{v} \cdot \boldsymbol{\Omega}$ replaced by total electron velocity, \mathbf{u} . Here \mathbf{u} is the sum (in the sense of Lorentz transformation) of the thermal velocity and the bulk velocity. We compute this 3-D integral numerically. Introducing a coordinate system with the z -axis along the bulk velocity and the x -axis along the direction of photon motion we obtain $\boldsymbol{\Omega} = (\sin\theta, 0, \cos\theta)$, where θ is the angle between $\boldsymbol{\Omega}$ and $\boldsymbol{\beta}$. Applying the Lorentz transformation we obtain the electron velocity in the disc frame,

$$\mathbf{u} = \left(\frac{v_x}{\gamma \left(1 + \beta \frac{v_x}{c}\right)}, \frac{v_y}{\gamma \left(1 + \beta \frac{v_x}{c}\right)}, \frac{v_z + \beta c}{1 + \beta \frac{v_x}{c}} \right), \quad (\text{A4})$$

with $\gamma = (1 - \beta^2)^{-1/2}$, and v_x , v_y and v_z – components of the electron’s thermal velocity. This enables to compute $\mathbf{u} \cdot \boldsymbol{\Omega}$ and calculate the required integral, which is now additionally a function of photon’s direction of motion, θ . We used the procedure `quad3d` from Press et al. (1992) to evaluate the integral.

The second modification concerns the scattering event. Since this is modeled in the electron rest frame, we introduced a pair of additional Lorentz transformations of a photon’s momentum: from the disc/corona frame to the frame comoving with the bulk velocity before simulating the scattering event, and the reverse transformation after the scattering event.

This paper has been processed by the authors using the Blackwell Scientific Publications L^AT_EX style file.